PEOPLE'S DEMOCRATIC REPUBLIC OF ALGERIAN
MINISTRY OF HIGHER EDUCATION & SCIENTIFIC RESEARCH

UNIVERSITY OF MOHAMED BOUDIAF - M'SILA

FACULTY OF TECHNOLOGY
DEPARTMENT OF ELECTRICAL ENGENERING
N° : ER-09

DOMAIN: SCIENCE AND TECHNOLOGY
STREAM : RENEWABLE ENERGY
OPTION : RENEWABLE ENERGIES IN ELECTRICAL ENGINEERING

Project Report Presented in Partial Fulfillment of the Requirements of the Degree Master

Presented by:

MERABET Zakaria

OUCIF Amir

Title

Numerical simulation analysis of a solar chimney power plant using ANSYS

Defended in front of the jury composed of:

First and last name	Grade	Establishment	Quality
Dr. HELLALI Lallouani	Assistant professor 'B'	University of M'sila	President
Dr. BAKRI Badis	Associate Professor 'A'	University of M'sila	Supervisor
Dr. BENGUESMIA Hani	Associate Professor 'A'	University of M'sila	Co- Supervisor
Dr. BOUAFIA Saber	Assistant professor 'B'	University of M'sila	Examiner

Academic year: 2023/ 2024

PEOPLE'S DEMOCRATIC REPUBLIC OF ALGERIAN
MINISTRY OF HIGHER EDUCATION & SCIENTIFIC RESEARCH

UNIVERSITY OF MOHAMED BOUDIAF - M'SILA

FACULTY OF TECHNOLOGY
DEPARTMENT OF ELECTRICAL ENGENERING
N° : ER-09

DOMAIN: SCIENCE AND TECHNOLOGY
STREAM : RENEWABLE ENERGY
OPTION : RENEWABLE ENERGIES IN ELECTRICAL ENGINEERING

Project Report Presented in Partial Fulfillment of the Requirements of the Degree Master

Presented by:

MERABET Zakaria

OUCIF Amir

Titled

Numerical simulation analysis of a solar chimney power plant using ANSYS

Defended in front of the jury composed of:

First and last name	Grade	Establishment	Quality
Dr. HELLALI Lallouani	Assistant professor 'B'	University of M'sila	President
Dr. BAKRI Badis	Associate Professor 'A'	University of M'sila	Supervisor
Dr. BENGUESMIA Hani	Associate Professor 'A'	University of M'sila	Co- Supervisor
Dr. BOUAFIA Saber	Assistant professor 'B'	University of M'sila	Examiner
Dr. DJERIOUI Ali	Professor	University of M'sila	Representative of the incubator/CATI
Mr. SAOUDI Mohammed	Engineer	Cosider Equipment Department -M'sila	Socio-economic partner

Academic year: 2023/ 2024

Acknowledgement

First and foremost, we thank God Allah, who gave us the courage, patience, strength, serenity, and will to complete this modest work during all these years of study.

The success of any project depends largely on the encouragement and guidance of many others. We take this opportunity to express our gratitude to the people who have been instrumental in the successful completion of this project.

Secondly, we would like to express our greatest appreciation to our supervisors, ***Dr. Badis Bakri,*** *Associate Professor at the University of M'sila, and* ***Dr. Hani Benguesmia****, Associate Professor at the University of M'sila.*

We can't say thank you enough for his tremendous support and help. We feel motivated and encouraged every time we attend his meetings. Without his encouragement and guidance, this Master's thesis would not have materialized

I would like to thank the president of the jury, ***Mr. Lallouani Hellali****, Associate at the University of M'sila, and the member of the jury,* ***Mr. Saber Bouafia****, Associate Professor at the University of M'sila, for having participated in the jury and for taking the time to examine my Master's thesis.*

Finally, I thank all those who contributed directly or indirectly to the development of this work especially ***Dr. Haythem Nasraoui,*** *Member at the laboratory LASEM at the University of sfax (ENIS),*

ملخص

يعد تقاطع المدخنة لمحطة توليد الطاقة الشمسية (SCPP) العنصر الرئيسي الذي يربط المجمع الشمسي بالمدخنة، مما يؤثر بشكل كبير على تصميم محطة توليد الطاقة الشمسية للمدخنة عن طريق تغيير اتجاه تدفق الهواء. تم استخدام الكود الرقمي "ANSYS Fluent" في هاته الدراسة لمعرفة كيفية تأثير نصف قطر تقاطع المدخنة على خصائص تدفق الهواء المحلي (الداخلي). تم فحص المتغيرات الديناميكية الحرارية مثل توزيع الضغط الكلي، وتوزيع درجة الحرارة، وتوزيع حجم السرعة لاثنين من الأجهزة مع أنصاف أقطار مختلفة لاتصال المدخنة. بالإضافة إلى ذلك، تم تحليل تأثير هذه العوامل على اضطراب الهواء في المنطقة الانتقالية. أظهرت النتائج أن التغييرات في نصف قطر الوصلة أثرت بشكل كبير على خصائص تدفق الهواء المحلي (الداخلي)، وبالتالي على كفاءة SCPP. علاوة على ذلك، تباينت السرعة القصوى داخل المدخنة وتغير موقعها مع تغير نصف قطر الوصلة. تؤثر هاته العوامل بشكل مباشر على الأداء العام للتوربين، مما يؤثر على كل من البنية والقدرة الطاقوية (الإستطـاعة).

الكلمات المفتاحية: الطاقة المتجددة، محطة توليد المدخنة الشمسية، نصف قطر الوصلة، تدفق الهواء المضطرب.

Abstract

The chimney junction of a Solar Chimney Power Plant (SCPP) is the main element connecting the solar collector to the chimney, significantly impacting the SCPP design by altering the airflow direction. This study utilized the numerical code "Ansys Fluent" to investigate how the chimney junction radius affects local airflow characteristics. The results showed that the local airflow characteristics and therefore the SCPP efficiency were significantly impacted by changes in junction radius. Additionally, the influence of these parameters on air turbulence in the transition zone was analyzed. The results demonstrated that changes in the junction radius significantly impacted local airflow characteristics and, consequently, the efficiency of the SCPP. Furthermore, the maximum velocity inside the chimney varied and shifted its location with changes in the junction radius. These factors directly affect the overall turbine performance, influencing both structure and power capacity.

Keyword: Renewable energy, solar chimney power plant, junction radius, turbulent airflow.

″List of Acronyms and Symbols″

List of Acronyms and Symbols

Symbols

c_p	Air's specific thermal capacity [$J.kg^{-1}K^{-1}$]
D_{ch}	Diameter of a chimney [m]
D_c	Diameter of the collector [m]
e	Thickness [mm]
g	Acceleration due to gravity [$m.s^{-2}$]
H_c	height of the collector [m]
H_{ch}	Height of the chimney [m]
I	Global radiation [$W.m^{-2}$]
k	Turbulent kinetic energy [$m^2.s^{-2}$]
P	Pressure [Pa]
Pr	Prandtl number [-]
r	Radial coordinate [m]
R_J	Junction radius [m]
t	Time [s]
T	Temperature [K]
u	Radial-direction velocity [-]
V	Air velocity [$m.s^{-1}$]
w	Tangentially directed velocity [$m.s^{-1}$]
z	Axial coordinate [m]

Greek symbols

β	Thermal expansion coefficient [-]
ε	Turbulent kinetic energy dissipation rate [$m^2.s^{-3}$]
μ	Dynamic viscosity [$m^2.s^{-1}$]
ρ	Density of the air [$Kg.m^{-3}$]

"List of Figures and Tables"

List of Figures and Tables

Chapter II: ″Numerical approach″

Chapter III: ″Results and discussion″

″Table of contents″

Table of contents

"General Introduction"

General Introduction

Coal, oil and natural gas have always been the energy sources on which human society has relied for centuries. These resources have been formed over millions of years, this is an inconvenient because it takes a long time. These fuels emit CO_2 gas that is harmful to the environment and toxicant which contribute global warming, air pollution and health issues.[1-3]

They also cause environmental degradation since their extraction usually involves destroying natural ecosystems where they are found, districting wildlife habitats and biodiversity on the other hand, is that their costs are unstable and thus often cause unpredictable effects on economies and family budgets. Fossil fuels still represent more than 80% of global energy production but cleaner energy sources gaining strength, around 29% by the end of 2020.over 50% of population in the world live in urban areas, after 30 years, it could be 70% where the electricity demand is expected to raise because of the technological advancements and the change of lifestyle. These concerns strongly emphasize the importance of moving to more sustainable, resilient and secure forms of energy to save our planet. In the face of environmental and economic challenges comforting the world today, the use of renewable energy is crucial to protect the environment and meet growing energy demands. Renewable energy and environmental protection are the pillars of sustainable development in the 21st century.[4-5]

These resources are characterized by the capacity of replenishment and low environmental impact. Its utilization involves a diverse range of technologies that tap into natural resources, including hydrological flows, geothermal heat, organic matter, wind velocity and solar irradiance.[6]

According to the IEA [International Energy Agency] in 2028, renewable energy sources account for over 42% of global energy production with the share of wind and solar PV doubling 25%. [7]

From the title, we can understand that the subject of our study revolves around solar energy, the solar chimney or solar updraft is a concept that falls under the category of solar thermal energy. it utilizes the greenhouse effect to generate an upward airflow which can be harnessed to produce electricity. it has a simple design compared to some other renewable energy

technologies, it consists of greenhouse, turbines and chimney. The scalability of solar chimney technology allows it to adapt different energy demands, small scale prototypes can be built for experimental purposes, while larger version could potentially generate significant amounts of electricity.[8]

The objective of this work is to establish out how the turbulent airflow within a solar chimney power plant is impacted by the chimney junction radius. Using the commercial program "ANSYS Fluent," the thermodynamic and turbulence characteristics are supplied for a number of settings. With the same chimney and collector dimensions, two-junction radius is investigated.

Specifically, the objectives can be outlined as follows; evaluate the Influence of Chimney Junction Radius, examine Turbine Site and Airflow Characteristics and Contribute to Renewable Energy Knowledge.

We have divided this work into three chapters to thoroughly understand the operation of solar chimney and delve deeper into its components.

In the opening chapter, we provided an overview of solar energy systems globally, with a particular focus on the solar chimney power plant. The literature review serves to contextualize our current research and validate the numerical and experimental findings we have obtained.

In the second chapter, In the second chapter, we present the governing equations and the numerical methods used in the commercial CFD code Ansys Fluent 16.2.

In the third chapter, numerical studies are presented to highlight the impact of radius of the junction on the flow characteristics within a solar chimney power plant.

Finally, we present a general conclusion and outlook suggests for this work.

Chapter I

″Literature review″

I.1. Introduction

Solar chimney power plants (SCPPs) represent an innovative approach to harnessing solar energy for electricity generation. This technology leverages the principles of convection to convert solar radiation into mechanical energy, which is then used to generate electrical power. The basic design of an SCPP consists of three main components: a large solar collector, a tall chimney, and turbines placed at the base of the chimney.

The concept of the solar chimney was first proposed by the German structural engineer Jörg Schlaich in the late 1970s. Since then, significant research and development efforts have been made to explore and optimize this technology. Solar chimneys offer several advantages, including the ability to generate power continuously (day and night) using stored thermal energy, a relatively simple construction with low maintenance requirements, and minimal environmental impact.[9]

This bibliography study aims to provide a comprehensive overview of the current state of research and development in the field of solar chimney power plants. It covers various aspects of SCPPs, including their design and components, theoretical foundations, operational performance, environmental impact, economic feasibility, and future prospects.

I.2. Historic

The concept of the solar chimney, also known as the solar updraft tower, has a rich history rooted in the early exploration of renewable energy technologies.

The idea of using solar energy to create an updraft for generating power dates back to the late 19th and early 20th centuries. One of the earliest mentions of the concept can be found in a 1903 article by the Spanish engineer Isidoro Cabanyes, who proposed the idea of a solar chimney to generate airflow for power production. However, it wasn't until several decades later that the concept began to gain more serious attention.[10]

In the 1930s, a German architect named Hermann Honnef envisioned a large-scale solar chimney power plant as a means to harness solar energy. Honnef's designs were ambitious, featuring tall towers intended to produce significant amounts of electricity. Despite the innovative nature of his ideas, technological and financial limitations of the time prevented these designs from being realized.

The first idea was accepted as the smoke jack by the Italian genius Leonardo daVinci (figure I.1.(a)). The idea of generating electricity from the sunlight was forward in 1903 by the Spanish

engineer Isidoro Cabanyes. He proposed a project of a solar motor, this machine consists of an air heater fixed to the house with a fireplace, inside the house a wind propeller was placed to generate electricity see figure I.1.(b).

In 1926, professor Bernard Dubos proposed to the French academy of sciences to build a solar aero electric power plant in north African Atlas Mountains. He filed his first patent in Algeria in 1956 called the tower to depression (Figure I.1.(c)).

It was artificially produces ancestry atmospheric vortex in a sort of round shaped haval nazzle.the military Edgard Nazare received a French patent for his invention in 1964.

In 1975, Robert Lucier made a patent application, which was accepted in 1981. The Manzanares, Spain prototype with 200m of height and 50 KW output was produced in 1982 by Jorg Schlaich (Figure I.1.(d)).

After this first realization of SC, scientists have given the importance to studies and research in the field.[11]

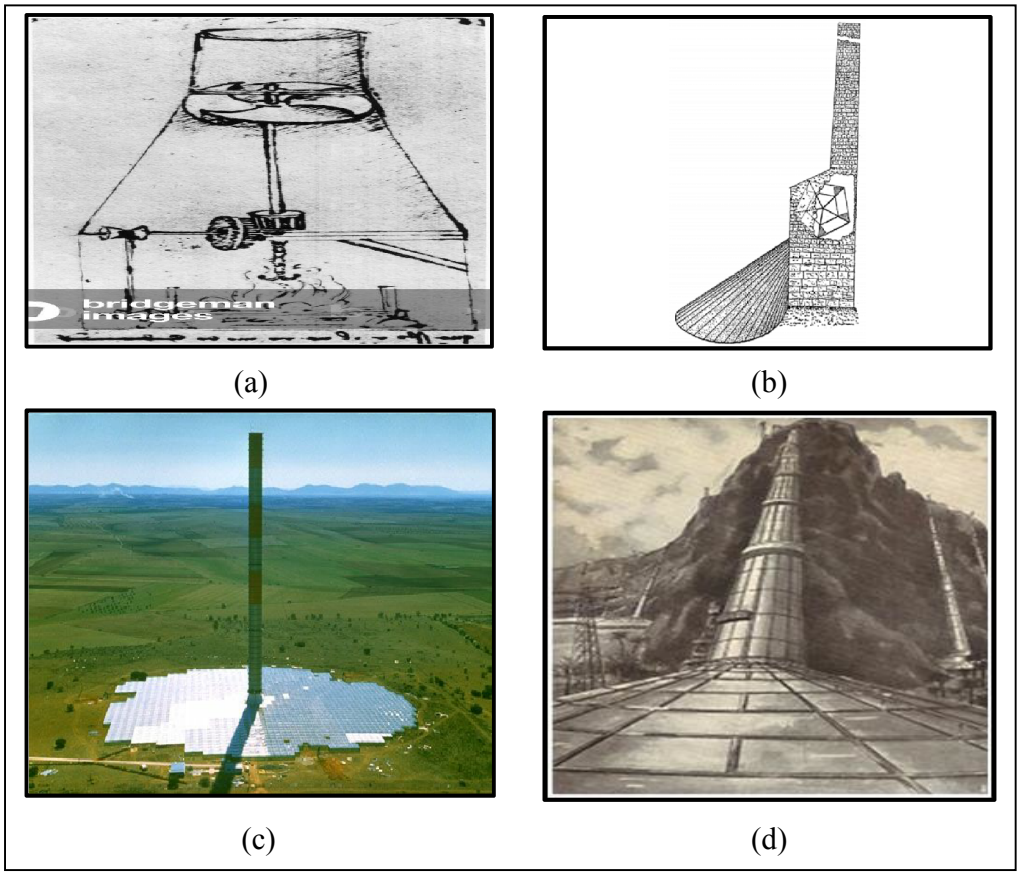

Figure I.1. The concept of the solar chimney.

I.3. Solar chimney definition

A solar chimney, also known as a solar updraft tower, is a type of renewable energy power plant that generates electricity by using solar energy to create a continuous airflow, which drives turbines connected to generators. The system relies on the natural convection of heated air to produce mechanical energy. [12]

The primary components of a solar chimney power plant include:

I.3.1. Solar Collector

A large, transparent or translucent circular area, usually made of glass or plastic, that absorbs solar radiation and heats the air beneath it. This area can span several kilometers in diameter. [12]

I.3.2. Chimney (Tower)

A tall, vertical structure situated at the center of the solar collector. The chimney height can range from hundreds to thousands of meters.

The heated air from the solar collector rises up through the chimney due to the difference in temperature between the hot air at the base and the cooler air at the top. [12]

I.3.3. Turbines

Positioned at the base of the chimney, these turbines are driven by the updraft of warm air rising through the chimney.

The mechanical energy from the turbines is then converted into electrical energy by connected generators. [12]

The process works as follows:

- Solar radiation heats the air under the solar collector,
- The heated air becomes less dense and rises towards the chimney,
- As the hot air moves upwards through the chimney, cooler air from the surroundings is drawn in to replace it, creating a continuous airflow,
- The airflow drives the turbines, generating electricity.

Solar chimneys are particularly suited to regions with high solar irradiance and vast expanses of land, such as deserts. They offer a sustainable and environmentally friendly method of power generation, with the potential for continuous operation day and night by utilizing thermal storage techniques. [12]

Overall, a solar chimney harnesses the principles of solar thermal energy and natural convection to produce renewable electricity, contributing to a diverse and sustainable energy portfolio.

Finally, the solar chimney is a straightforward and low maintenance technology designed to generate electricity it operates by harnessing the kinetic energy produced when sunlight heats air, causing it to rise vertically through a chimney. This upward movement of air powers a turbine generator, converting the energy into electricity. While it primarily functions during the day using solar radiation, it can continue operating at night by utilizing a thermal storage system.

Figure I.2. Solar chimney power plant.

I.4. Solar chimney components

A solar chimney, also known as a solar updraft tower, consists of three main components: the solar collector, the chimney (or tower), and the turbines. Each component plays a crucial role in the overall operation and efficiency of the system. [13]

I.4.1. Solar Collector

The solar collector is the component responsible for capturing solar energy and heating the air. It is a large cover with transparent materials such as plastic or glass which help to absorb the sun radiation ,the larger is the surface area the greater energy produced by the solar tower .This cover is supported by a matrix extending horizontally for an optimized distance, holding it in place above the ground. This support is designed to distribute the weight of collector, it can be metal or reinforced plastics. (figure I.3). [1]

The periphery of collector in the center is directly connected to the base of the tower .This connection allows the heated air absorbed by the cover to be diverted into vertical movement with minimal loss of friction. Whereas it is open to the surrounding environment. This cover admits the components of short wave solar radiation and retains the long wave radiation from the ground. Thus, the ground under the collector heats up and transfers its heat to the air flowing radially from outside to the tower. The most efficient collector s material is the glass, where it can convert more than 70% of solar energy into heat. The annual average is around 50%, with maintenance and proper care it lasts 60 years or plus.

- **Design:** It is typically a large, transparent or translucent circular area made of glass or plastic that covers several kilometers in diameter.
- **Function:** The collector absorbs solar radiation, which heats the air beneath it. The design ensures that the maximum amount of solar energy is captured and converted into thermal energy.
- **Construction:** The collector is elevated slightly above the ground to allow the cooler air to enter from the edges and flow towards the center as it heats up. [12]

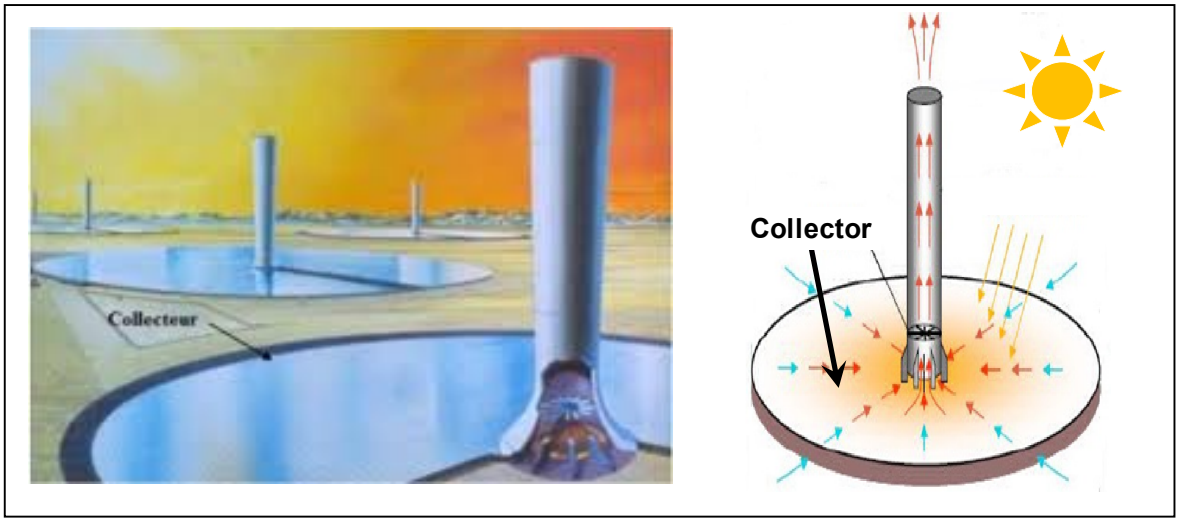

Figure I.3. Solar collector

I.4.2. Turbine

The turbines are the mechanical components that convert the kinetic energy of the moving air into electrical energy. (Figure I.4).

- **Design:** The turbines are placed at the base of the chimney where the airspeed is highest.

- **Function:** As the heated air rises through the chimney, it drives the turbines. The mechanical energy from the turbines is then converted into electrical energy by connected generators.
- **Construction:** Turbines are designed to operate efficiently with low wind speeds and are typically robust to handle continuous operation. [12]

The turbine is the important part of this construction, where it transfers the kinetic energy of the warm air of the system with difference of pressure created by the chimney to thermal energy.

Also, the turbine could be installed in the center of collector in different positions, usually one turbine is used inside a chimney at a certain height parallel to the ground .figure 1.4.

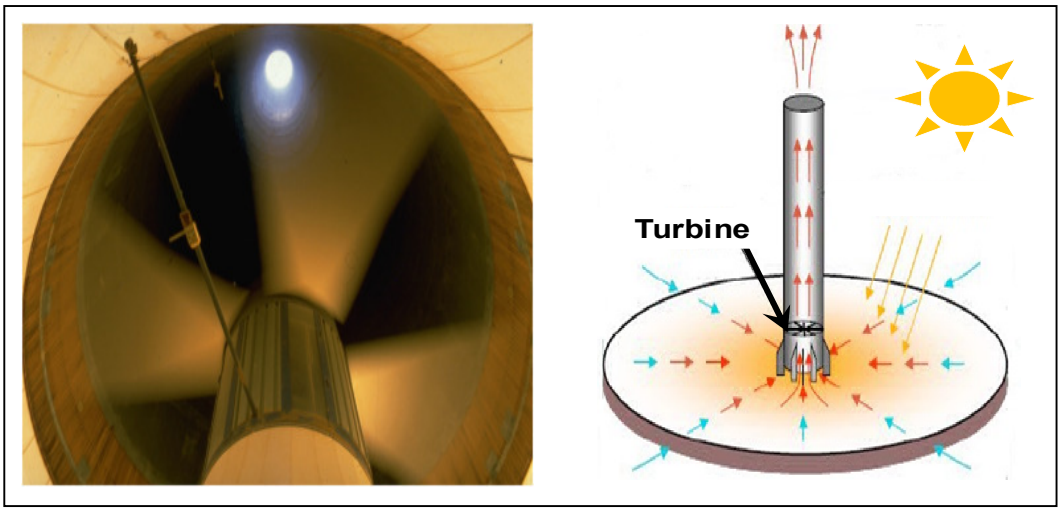

Figure I.4. Turbine.

I.4.3. Chimney (Tower)

The chimney is a tall, vertical structure where the heated air rises, creating a continuous airflow.

- **Design:** The chimney can range from hundreds to thousands of meters in height. The height is critical as it influences the airflow speed and the overall efficiency of the system.
- **Function:** The chimney uses the temperature difference between the hot air at the base and the cooler air at the top to drive the upward movement of air. This natural convection process is the key to generating the kinetic energy needed to power the turbines.
- **Construction:** It is usually made of durable materials that can withstand high temperatures and environmental conditions. The inside of the chimney is designed to minimize air resistance and maximize airflow. [12]

The tower is the central feature of a solar chimney, installed at the center of the collector. It acts as the system's motor, creating a temperature differential between the cold air at the top and the heated air at the bottom. This temperature difference, along with the pressure difference caused by the height, generates a vacuum effect in the center of the roof. The tower's height can pose structural challenges and potential dangers due to environmental factors post-construction, necessitating a stable base that allows free airflow through the turbine. The tower is typically constructed from concrete or steel, rather than lightweight materials. [14]

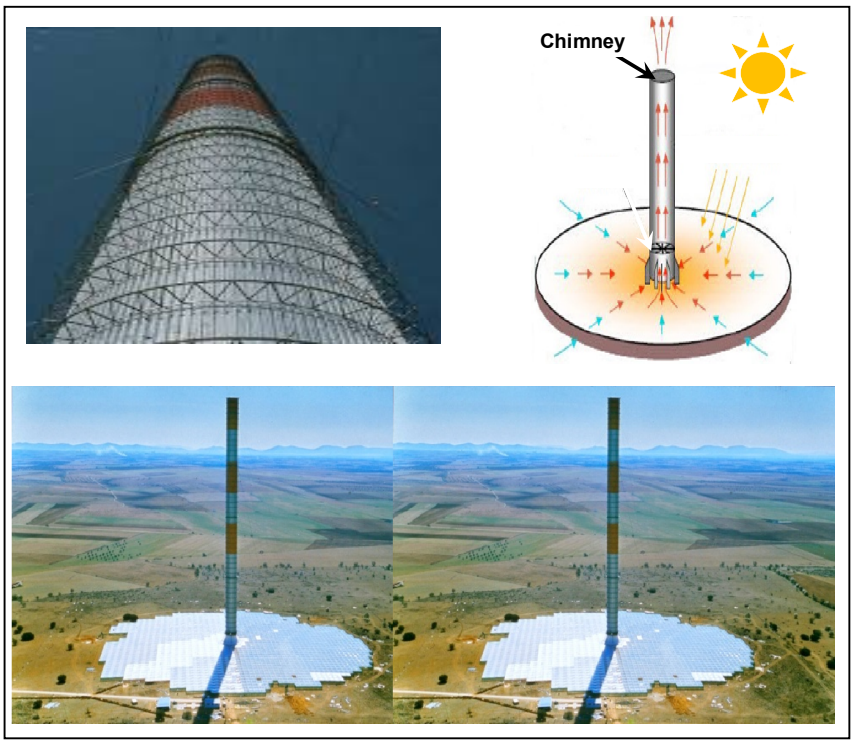

Figure I.5. Chimney (Tower).

Note: The chimney in manzanares,spain made of sheet steel rings supported by guyed wires.

I.5. Principle of operation of the solar chimney

The solar chimney power plant operates by leveraging solar energy to heat air, creating an updraft through a tall chimney. This updraft drives turbines, which generate electricity. The system can operate continuously with the aid of a thermal storage system, making it a viable solution for sustainable and renewable energy generation.

The design takes advantage of natural convection and pressure differentials to convert solar energy into usable electrical power efficiently. (Figure I.5). [15]

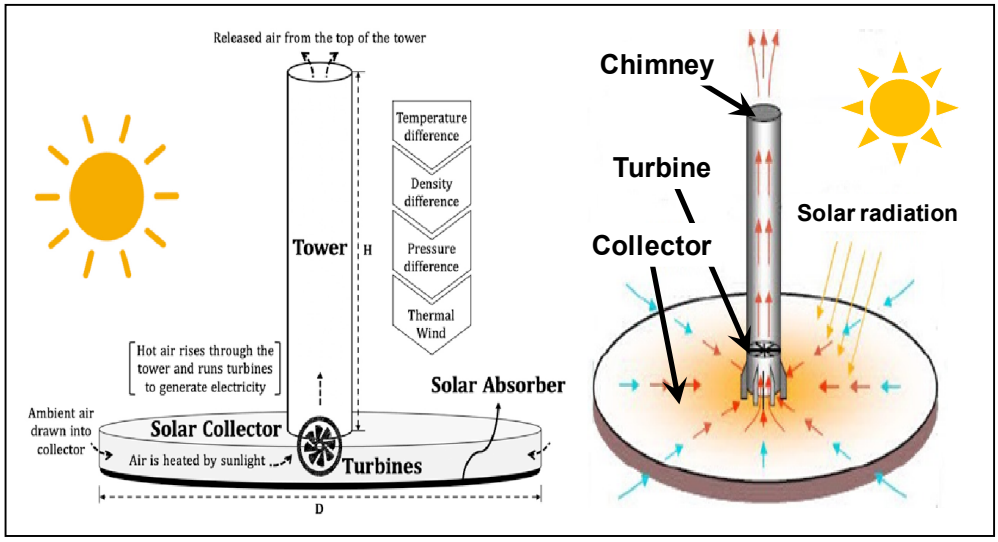

FigureI.6. Schematic view of solar chimney working principle.

I.6. Advantages and disadvantages solar chimney power plant

Certainly, here's a breakdown of the advantages and disadvantages of solar chimney power plants:

I.6.1. Solar chimney advantages

- Solar chimneys utilize solar energy, which is renewable and abundant, reducing reliance on finite fossil fuels,
- Once constructed, solar chimney power plants have low operational and maintenance costs compared to traditional fossil fuel power plants,
- Solar chimneys can generate electricity continuously, even during periods of low sunlight or at night, by utilizing thermal storage systems,
- Solar chimneys produce electricity without emitting greenhouse gases or pollutants, contributing to reduced air pollution and mitigating climate change,
- The technology behind solar chimneys is relatively simple and straightforward, with fewer moving parts compared to other renewable energy systems, resulting in lower maintenance requirements,
- Solar chimney power plants can be scaled up or down to meet varying energy demands, making them adaptable to different locations and power requirements,
- Exploitation of direct and diffuse solar radiations,
- Does not require water,

- Low cost materials,
- Production of electricity 24h/24h,
- With minimal maintenance, it is expected to last 80 years,
- No fuel is needed,
- There is no gas emission, so it does not present risk of pollution to the environment,
- Simple fully automatic operation,
- The construction is easy in the desert regions, while utilizing sand to develop the primary construction materials, such as glass and concrete. [16]

I.6.2. Solar chimney disadvantages

- The construction of solar chimney power plants requires significant upfront capital investment due to the large-scale infrastructure involved, such as the chimney and solar collector, (It requires high initial investment cost),
- Solar chimneys require large areas of land for the solar collector, which could compete with other land uses such as agriculture or conservation,
- Building and maintaining tall chimneys present engineering challenges, including structural integrity and safety concerns, especially in areas prone to extreme weather events,
- Solar chimneys have relatively low efficiency compared to other renewable energy technologies like solar photovoltaic panels or wind turbines, which may limit their widespread adoption,
- Solar chimneys perform best in regions with high solar radiation and clear skies, limiting their viability in areas with less consistent sunlight or frequent cloud cover,
- The large, imposing structures of solar chimneys may have visual impacts on the landscape, potentially affecting local aesthetics and land use,
- The collector needs a large surface,
- The production is not stable during the day or the year,
- The massive structure requires a lot of expertise in engineering.

Finally, while solar chimneys offer numerous advantages such as renewable energy generation, low operating costs, and environmental benefits, they also face challenges like high initial investment, land use requirements, and efficiency concerns. Balancing these factors is essential when considering the implementation of solar chimney power plants as part of a sustainable energy strategy. [16]

I.7. Manzanares prototype

The first prototype of a solar chimney power plant was built in 1982 in Manzanares Ciudad Real,150 km south of Madrid Spain.

The project was led by a team of engineers and researchers, with support from the German government and the Spanish government's National Institute for Energy Diversification and Saving (IDAE).

However, this power plant worked just for seven years due to the corrosion of the unprotected guy wires of the tower, which rusted and collapsed during the storm. This caused the tower to fall over, and the plant was taken out of service in 1989 inexpensive materials were used to evaluate their performance.

The solar tower was built of iron plating only 1.25 mm thick under the direction of a German engineer, Jorg Schlaich , funded by the German government . the technical data of this prototype are compiled in the table I.1.

Table I.1. The technical data of Manzanares solar chimney prototype.

Chimneyheight	194.6 m
Chimney diameter	10.16 m
Chimney weight	125
Collector diameter	244 m
Collector radius	122 m
Collector height	1.85 m
Collector area with membrane	40 000 m^2
Collector area with glass	6000 m^2
Power output	**50 kW**
Number of turbine blades	**4**
Turbine blade profile	FX W-151-A
The collector temperature difference ΔT	20 °C
Operation modes	Stand-alone or grid connected mode

Figure I.7. Solar chimney power plant of Manzanares, Spain

I.8. The Arizona project

Enviro Mission, an Australian firm renowned for its innovative approach to renewable energy, is currently spearheading a groundbreaking technological endeavor in the vast expanse of the Arizona desert. Collaborating closely on this ambitious project is Faithful and Gould, a prominent North American construction consulting firm.

Their mission is to construct a massive 200 MW solar power tower capable of providing sustainable energy to approximately 150,000 American households. This endeavor represents a significant step forward in the quest for clean and reliable power sources. What sets this project apart, according to its designers, is its remarkable longevity and minimal maintenance requirements. With an anticipated continuous energy generation span of 80 years, the solar tower promises to be a sustainable solution for decades to come.

Furthermore, the Southern California Public Power Authority has already committed to purchasing the electricity generated by Enviro Mission's tower for the next three decades, solidifying its economic viability and long-term impact on the region’s energy landscape.[17]

The concept is that it uses the daily generation of warm air at the surface by the sun to generate electricity. It takes the familiar principle of a chimney filled with buoyant, hot air to the extreme. The taller and wider the tower, and the hotter the air it contains, the greater the potential for energy generation. The solar heated air in the tower continuously draws air into the 2.5+ mile wide glass/plastic canopy and through approximately 32 wind turbines, each rated at 6.25 MW, circling the base of the tower.[17]

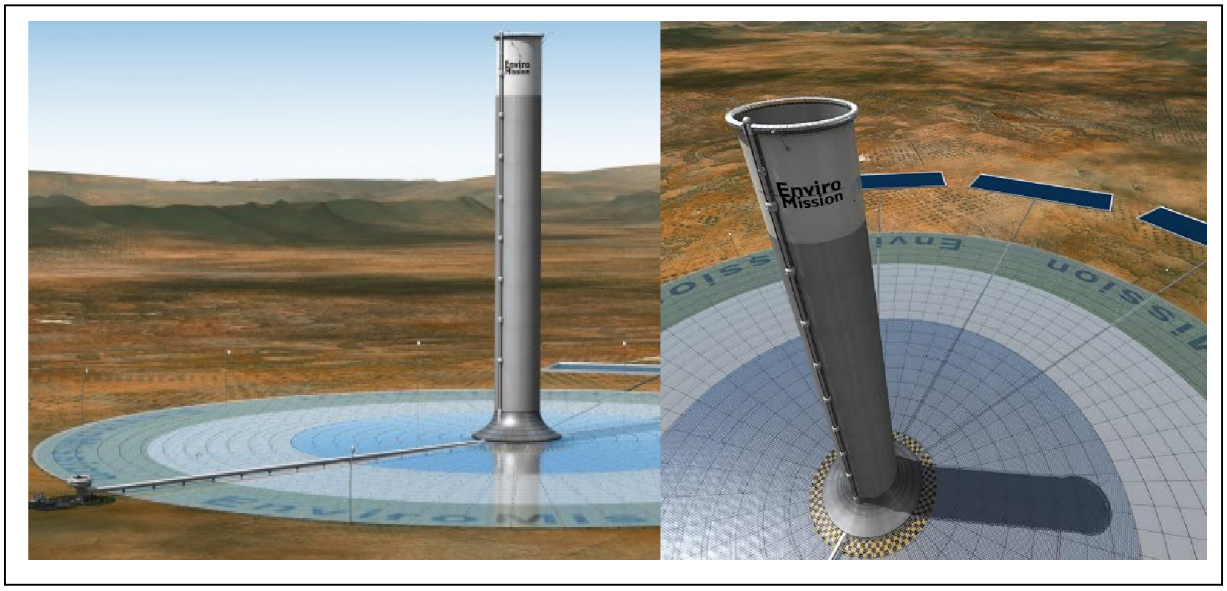

Figure I.8. The American project Arizona.

I.9. Conversion rate of solar energy to electrical energy

The solar updraft tower is a type of solar power plant that generally has a lower efficiency in converting solar energy to electricity compared to other solar thermal technologies.

Typically, it achieves about 0.5% efficiency, which is substantially lower than the 20% to 31.25% seen in concentrated solar power CSP or concentrated photovoltaic CPV systems. However, the investment cost per square meter of the solar collecting area for updraft towers is quite low, partially offsetting their lower efficiency.

For instance, a 100 MW solar updraft tower would require a chimney 1000 meters tall and a greenhouse covering 20 km^2, while a 200 MW facility would need a greenhouse 7 kmin diameter, covering approximately 38 $km^{2.}$ Such a plant could power about 200 000 homes and reduce gas emissions by over 900 000 tones each year.

Despite its modest efficiency, the design allows for versatile land use, potentially integrating agricultural activities or additional solar installations under the vast area of the greenhouse. Challenges such as atmospheric winds, structural drag, and reflective losses can affect the performance of these towers.

The large land requirement and low efficiency are critical considerations when evaluating the viability of solar updraft towers against other solar technologies.

I.10. Conclusion

The history of the solar chimney is a testament to the enduring appeal and potential of harnessing solar energy through innovative means. From early theoretical concepts to modern pilot projects and research initiatives, the development of solar chimney technology reflects the continuous quest for clean and renewable energy solutions. As technological advancements continue and the urgency of addressing climate change grows, solar chimneys may yet play a significant role in the global energy landscape. The next chapter presents a numerical approach of the SCPP.

Chapter II

″Numerical approach″

II.1. Introduction

The concept of Solar Chimney Power Plants (SCPPs) revolves around harnessing solar energy to generate electricity through natural convection and airflow.

It is represents a promising renewable energy technology that harnesses solar energy to produce electricity.

The fundamental principle involves creating a controlled environment where solar energy is used to heat air, which then rises through a tall chimney, driving turbines to generate power.

Given the complexity of this system, numerical modeling and simulation are crucial for understanding and optimizing the performance of SCPPs.[1]

The subsequent sections from this chapter will delve into the equations and models utilized by Ansys Fluent 16.2 to simulate a solar chimney power plant.

II.2. Components of a Solar Chimney Power Plant

A Solar Chimney Power Plant (SCPP) harnesses solar energy to generate electricity through a combination of greenhouse and chimney effects. The main components of an SCPP are:[1,5]

II.2.1. Solar Collector

The solar collector is a large, transparent roof structure that covers a wide area. It traps solar radiation and heats the air underneath it. The heated air becomes buoyant and starts to rise towards the chimney.

II.2.2. Chimney

The chimney, or tower, is a tall vertical structure through which the heated air rises. The height of the chimney is critical as it directly influences the pressure difference and, consequently, the airflow speed.

II.2.3. Turbines

Located at the base of the chimney, turbines convert the kinetic energy of the rising air into mechanical energy, which is then transformed into electrical energy by generators.

II.3. Importance of Numerical Modeling

Numerical modeling plays a vital role in the design and analysis of SCPPs. It allows for the simulation of complex physical processes, including: [12]

II.3.1. Heat Transfer

The absorption of solar radiation and its conversion into thermal energy within the solar collector.

II.3.2. Fluid Dynamics

The behavior of air as it flows from the collector through the chimney, influenced by buoyancy effects and pressure gradients.

II.3.3. Turbulence

The impact of turbulent air flow, which is significant in determining the efficiency of the power plant.

II.3.4. Energy Conversion

The efficiency of turbines in converting kinetic energy of air into electrical energy.

II.4. Objectives of Numerical Modeling

Numerical modeling of a Solar Chimney Power Plant (SCPP) serves several critical objectives aimed at improving the understanding, design, and performance of these systems. Here are the primary objectives:[12]

II.4.1. Performance Prediction

Estimate the power output and efficiency of the SCPP under various operational conditions.

II.4.2. Optimization

Identify optimal design parameters such as collector size, chimney height, and turbine placement to maximize efficiency.

II.4.3. Feasibility Studies

Assess the viability of implementing SCPPs in different geographic locations with varying solar irradiance levels.

II.4.4. Cost-Benefit Analysis

Evaluate the economic aspects by analyzing construction, maintenance costs, and expected energy yield.

II.5. Modeling Approach

To achieve these objectives, the modeling approach typically involves the following steps: [18-19]

II.5.1. Mathematical Formulation

Develop governing equations based on principles of conservation of mass, momentum, and energy. These equations are usually partial differential equations (PDEs) that describe fluid flow and heat transfer.

II.5.2. Discretization

Convert the continuous PDEs into discrete forms using numerical methods such as Finite Volume Method (FVM), Finite Difference Method (FDM), or Finite Element Method (FEM).

II.5.3. Simulation Setup

Define the geometry of the SCPP, generate a computational mesh, and apply boundary and initial conditions.

II.5.4. Solver Implementation

Use computational fluid dynamics (CFD) software to solve the discretized equations. Popular CFD tools include ANSYS Fluent, OpenFOAM, and COMSOL Multiphysics.

II.5.5. Validation and Verification

Validate the model against experimental data or analytical solutions to ensure accuracy. Verification ensures the numerical model is solving the equations correctly.

II.5.6. Analysis and Interpretation

Analyze the results to understand the flow characteristics, temperature distribution, and overall performance of the SCPP. Use these insights to make design improvements.

II.6. Mathematical formulation

The mathematical formulation of a Solar Chimney Power Plant (SCPP) involves developing and solving a set of governing equations that describe the physical processes of fluid flow and heat transfer within the system.

These equations are derived from the principles of conservation of mass, momentum, and energy.

Implementing all of the above simplifications, the fundamental equations become: [20-23]

- **The continuity equation**

$$\vec{\nabla}.\rho\vec{V} = 0 \qquad \text{(II.1)}$$

- **The momentum equations**

$$\frac{d\rho\vec{V}}{dt} + (\vec{V}.\vec{\nabla}).\vec{V} = -\frac{1}{\rho_0}.\vec{\nabla}p + \frac{\mu}{\rho_0}.\vec{\nabla}.(\vec{\nabla}.\vec{V}) + \vec{g}.(1 - \beta(T - T_0)) \qquad \text{(II.2)}$$

- **The energy conservation equation**

$$\frac{d\rho CpT}{dt} + \vec{\nabla}.\rho CpT\vec{V} = \vec{\nabla}.(\lambda\vec{\nabla}T) \qquad \text{(II.3)}$$

$$\frac{dT}{dt} + \vec{\nabla}T.\vec{V} = \alpha\,\vec{\nabla}.\vec{\nabla}T \qquad \text{(II.4)}$$

Where:

$$\alpha = \frac{\lambda}{\rho c_p} \qquad \text{(II.5)}$$

These equations do not have an analytic solution; therefore usually it used simplification of these to achieve an approximate solution. The dimensionless number is used to carry out these simplifications, as the Reynolds number or the Rayleigh number.

The Reynolds number gives a measure of the ratio of inertial forces to viscous forces and consequently quantifies the relative importance of these two types of forces for given flow conditions:

❖ When this number is high (Re>>1) the viscous forces can be neglected.

❖ Also, when Re<2300 in ducts, a laminar flow occurs and for Re>4000 the flow is turbulent.

II.7. Computational Fluid Dynamics (CFD)

Computational Fluid Dynamics (CFD) is a powerful tool used to analyze and solve problems involving fluid flows and heat transfer through numerical simulations. CFD is particularly useful in the design and optimization of Solar Chimney Power Plants (SCPPs) due to the complex interactions between the airflow and thermal processes.

- Computational Fluid Dynamics (CFD) has become a widely adopted methodology for solving complex fluid flow problems in fluid mechanics and heat transfer and an important tool

in chemical and process engineering. With increasing industrial competitiveness and a focus on sustainability, industries are compelled to reduce time-to-market while designing more energy-efficient, safer, and flexible processes with lower emissions. CFD is particularly useful for exploring new and improved process designs, enabling the investigation of various design possibilities and reducing inefficiencies such as recirculation zones, which can diminish process efficiency.[12]

- The fundamental laws of mechanics applied to a fluid yield the governing equations for fluid flow. These equations, together with the conservation of energy equation, form a set of coupled, nonlinear partial differential equations. Solving these equations analytically is impractical for most engineering problems; however, approximate solutions can be obtained using computer-based methods, which is the essence of CFD.
- CFD is based on the Navier-Stokes equations, which describe the relationships between the velocity, pressure, temperature, and density of a moving fluid. By modeling these equations, CFD helps identify hot spots and areas where cold air is wasted or air is mixing inefficiently.
- There are many CFD software options available, and in this context, we use Ansys Fluent 16.2 to model the airflow in the solar chimney.[21]
- Several commercial CFD codes are available for solving numerical equations, many of which feature a graphical user interface to facilitate user-friendly simulation setup. Examples of these commercial CFD codes, and Flow-works Simulation.

Once a suitable simulation program is selected, the flow problem must be modeled, starting with pre-processing and concluding with post-processing of the numerical simulation. The general structure of flow modeling, as illustrated in Figure II.1, can be divided into three main steps (pre-processing, solving, and post-processing).

- To numerically solve the partial differential equations, we will discretize them to obtain a system of algebraic equations. Several discretization methods are well-known, including the Finite Volume Method (FVM), Finite Element Method (FEM), and Finite Difference Method (FDM). The Fluent code frequently utilizes the Finite Volume Method (FVM).
- The Fluent code frequently utilizes the Finite Volume Method (FVM) due to its effectiveness in accurately modeling fluid flows and heat transfer phenomena. FVM is particularly well-suited for complex geometries and unstructured meshes, making it versatile for a wide range of engineering applications.

Additionally, FVM inherently conserves mass, momentum, and energy within control volumes, ensuring robust and reliable simulations. [23]

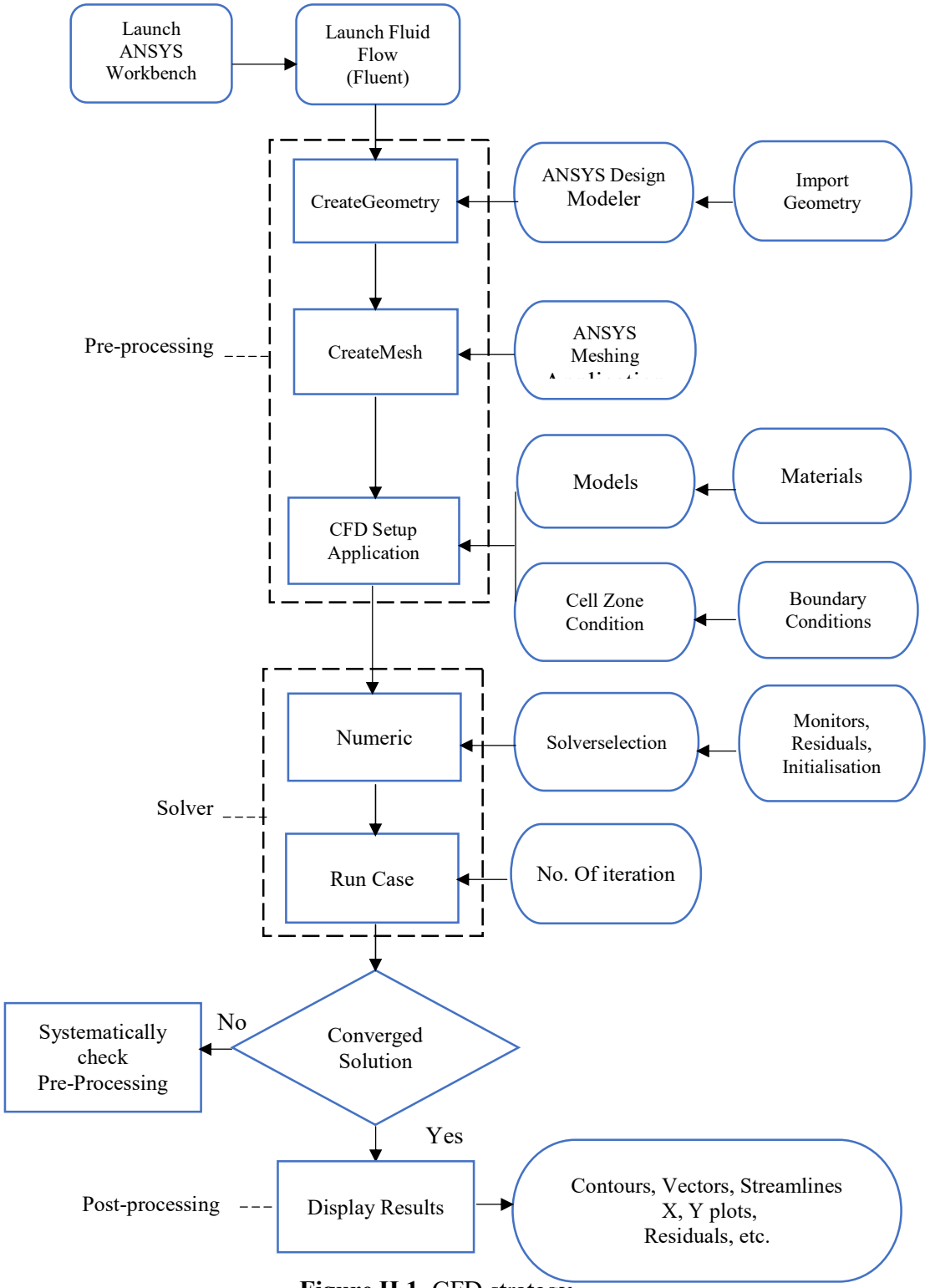

Figure II.1. CFD strategy.

II.8. Turbulent models

Turbulent models in Computational Fluid Dynamics (CFD) are mathematical representations used to simulate the effects of turbulence in fluid flow. Turbulence, characterized by chaotic and unpredictable fluid motion, plays a significant role in many engineering applications, including aerodynamics, heat transfer, and combustion. Several turbulent models are available, each with its own level of complexity and applicability to different flow regimes and geometries. Here are some commonly used turbulent models: [12,18]

II.8.1. k-ε (K-Epsilon) Model

A two-equation model that solves for the turbulent kinetic energy (k) and its dissipation rate (ε). It is one of the most commonly used turbulent models due to its robustness and computational efficiency. It is suitable for a wide range of turbulent flows, including wall-bounded and free shear flows.

The standard k-ε model is one of the most common turbulence models, although it just does not perform well in cases of large adverse pressure gradients. It is a two-equation model and includes two extra transport equations to represent the turbulent properties of the flow.

This allows a two equation model to account for history effects like convection and diffusion of turbulent energy.

The first transported variable is the turbulent kinetic energy k. The second transported variable in this case is the dissipation rate of the turbulent kinetic energy. It is the variable that determines the scale of the turbulence, whereas the first variable k determines the energy in the turbulence.
The standard k-ε model is one of the most widely used turbulent models in Computational Fluid Dynamics (CFD).

It is a two-equation turbulence model that solves for two transport equations: one for the turbulent kinetic energy (k) and another for the rate of dissipation of turbulent kinetic energy (ε).

$$\frac{\partial}{\partial t}(\rho k) + \frac{\partial}{\partial x_i}(\rho k u_i) = \frac{\partial}{\partial x_j}\left[\left(\mu + \frac{\mu_t}{\sigma_k}\right)\frac{\partial k}{\partial x_j}\right] + G_k + G_b - \rho\varepsilon - Y_M + S_k \qquad \text{(II.6)}$$

And

$$\frac{\partial}{\partial t}(\rho \varepsilon) + \frac{\partial}{\partial x_i}(\rho \varepsilon u_i) = \frac{\partial}{\partial x_j}\left[\left(\mu + \frac{\mu_t}{\sigma_\varepsilon}\right)\frac{\partial \varepsilon}{\partial x_j}\right] + \frac{\varepsilon}{k}C_{1\varepsilon}(G_k + C_{3\varepsilon}G_b) - C_{2\varepsilon}\rho\frac{\varepsilon^2}{k} + S_\varepsilon \qquad \text{(II.7)}$$

Where:

G_k: generation of turbulence kinetic energy due to the mean velocity gradients, calculated as described in modeling turbulent production in the k-ε models.

G_b: generation of turbulence kinetic energy due to buoyancy, calculated as described in effects of buoyancy on turbulence in the k-ε Models.

Y_M: contribution of the fluctuating dilatation in compressible turbulence to the overall dissipation rate, calculated as described in effects of compressibility on turbulence in the k- ε models.

$C_{1\varepsilon}$, $C_{2\varepsilon}$and $C_{3\varepsilon}$ are constants. $\sigma_k$and $\sigma_\varepsilon$are the turbulent Prandtl numbers for k and ε respectively.

S_k and S_ε are user-defined source terms.

The turbulent (or eddy) viscosity μ_t is computed by combining k and ε as follows:

$$\mu_t = \rho C_\mu \frac{k^2}{\varepsilon} \qquad \text{(II.8)}$$

Constants of the Standard k-ε model are presents in table II.1.

Table II.1. Constants of the standard k-ε model.

$C_{1\varepsilon}$	$C_{2\varepsilon}$	C_μ	σ_k	σ_ε
1.44	1.92	0.09	1.0	1.3

The realizable $k-\varepsilon$ (k-epsilon) model is an enhanced version of the standard $k-\varepsilon$ turbulence model that addresses some of its limitations. Developed by Shih et al., the realizable $k-\varepsilon$ model aims to improve the accuracy and reliability of predictions for a wider range of turbulent flows.

To understand the mathematics behind the realizable k-ε model, consider combining the Boussinesq relationship and the eddy viscosity definition to obtain the following expression for the normal Reynolds stress in an incompressible strained mean flow:

$$\overline{u^2} = \frac{2}{3}k - 2\nu_t \frac{\partial U}{\partial x} \qquad \text{(II.9)}$$

Using equation (II.3) for $\nu_t \equiv \mu_t/\rho$, we obtain the result that the normal stress, $\overline{u^2}$, which by definition is a positive quantity, becomes negative, that is, “non-realizable”, when the strain is large enough to satisfy:

$$\frac{k}{\varepsilon}\frac{\partial U}{\partial x} > \frac{1}{3C_\mu} \approx 3.7 \qquad \text{(II.10)}$$

Similarly, it can also be shown that the Schwarz inequality for shear stresses ($\overline{u_\alpha}\overline{u_\beta^2} \le \overline{u_\alpha^2}\overline{u_\beta^2}$; no summation over α and β) can be violated when the mean strain rate is large.

The most straightforward way to ensure the realizability (positivity of normal stresses and Schwarz inequality for shear stresses) is to make, C_μ variable by sensitizing it to the mean flow (mean deformation) and the turbulence (k,ε).

The notion of variable C_μ is suggested by many modelers including Reynolds, and is well substantiated by experimental evidence.

For example, C_μ is found to be around 0.09 in the logarithmic layer of equilibrium boundary layers, and 0.05 in a strong homogeneous shear flow.

The modeled transport equations for k and εin the realizable k-ε model are:

$$\frac{\partial}{\partial t}(\rho k) + \frac{\partial}{\partial x_j}(\rho k u_j) = \frac{\partial}{\partial x_j}\left[\left(\mu + \frac{\mu_t}{\sigma_k}\right)\frac{\partial k}{\partial x_j}\right] + G_k + G_b - \rho\varepsilon - Y_M + S_k \qquad \text{(II.11)}$$

$$\frac{\partial}{\partial t}(\rho\varepsilon) + \frac{\partial}{\partial x_j}(\rho\varepsilon u_j) = \frac{\partial}{\partial x_j}\left[\left(\mu + \frac{\mu_t}{\sigma_\varepsilon}\right)\frac{\partial \varepsilon}{\partial x_j}\right] + \frac{\varepsilon}{k}C_{1\varepsilon}C_{3\varepsilon}G_b + \rho C_1 S_\varepsilon - C_2\rho\frac{\varepsilon^2}{k+\sqrt{v\boldsymbol{\varepsilon}}} + S_\varepsilon \qquad \text{(II.12)}$$

Where:

$$C_1 = \max\left[0.43, \frac{\eta}{\eta+5}\right] \qquad \text{(II.13)}$$

$$\eta = S\frac{k}{\varepsilon} \qquad \text{(II.14)}$$

$$S = \sqrt{2\,S_{ij}S_{ij}} \qquad \text{(II.15)}$$

As in other k-ε models, the eddy viscosity is computed from:

$$\mu_t = \rho C_\mu \frac{k^2}{\varepsilon} \qquad \text{(II.16)}$$

The difference between the realizable k-ε model and the standard and RNG k- ε models is that is no longer constant. It is computed from:

$$C_\mu = \frac{1}{A_0 + A_s\frac{kU^*}{\varepsilon}} \qquad \text{(II.17)}$$

Where:

$$U^* \equiv \sqrt{S_{ij}S_{ij} + \widetilde{\Omega}_{ij}\widetilde{\Omega}_{ij}} \quad \text{(II.18)}$$

And

$$\widetilde{\Omega}_{ij} = \Omega_{ij} - 2\,\varepsilon_{ijk}w_k \quad \text{(II.19)}$$

$$\Omega_{ij} = \widetilde{\Omega}_{ij} - \varepsilon_{ijk}w_k \quad \text{(II.20)}$$

Where $\widetilde{\Omega}_{ij}$ is the mean rate-of-rotation tensor viewed in a moving reference frame with the angular velocityw_k.

The model constants A_0 and A_s are given by:

$A_0 = 4.04$,

$$A_s = \sqrt{6}\cos\emptyset$$

Where:

$$\emptyset = \frac{1}{3}\cos^{-1}\left(\sqrt{6}W\right) \quad \text{(II.21)}$$

$$W = \frac{S_{ij}S_{jk}S_{ki}}{\tilde{S}^3} \quad \text{(II.22)}$$

$$\tilde{S} = \sqrt{S_{ij}S_{ij}} \quad \text{(II.23)}$$

$$S_{ij} = \frac{1}{2}\left(\frac{\partial u_j}{\partial x_i} + \frac{\partial u_i}{\partial x_j}\right) \quad \text{(II.24)}$$

The constants of the Realizable k-ε model is presented in table II.2.

Table II.2. Constants of the standard k-ε model.

$C_{1\varepsilon}$	C_2	σ_k	σ_ε
1.44	1.9	1.0	1.2

The RNG $k-\varepsilon$ (k-epsilon) model is a variant of the standard $k-\varepsilon$ turbulence model that incorporates modifications based on the Renormalization Group (RNG) theory. Developed by Yakhot and Orszag, the RNG $k-\varepsilon$ model aims to improve the accuracy and robustness of turbulence predictions, particularly in complex flow situations.

The RNG k-ε model was derived using a statistical technique called renormalization group theory.

It is similar in form to the standard k-ε model, but includes the following refinements:

❖ The RNG model has an additional term in its ε equation that improves the accuracy for rapidly strained flows.

❖ The effect of swirl on turbulence is included in the RNG model, enhancing accuracy for swirling flows.

❖ The RNG theory provides an analytical formula for turbulent Prandtl numbers, while the standard k-εmodel uses user-specified, constant values. While the standard k-ε model is a high-Reynolds number model, the RNG theory provides an analytically derived differential formula for effective viscosity that accounts for low-Reynolds number effects. Effective use of this feature does, however, depend on an appropriate treatment of the near-wall region. These features make the RNG k-ε model more accurate and reliable for a wider class of flows than the standard k-ε model.

The RNG-based k-ε turbulence model is derived from the instantaneous Navier-Stokes equations, using a mathematical technique called "renormalization group" (RNG) methods. The analytical derivation results in a model with constants different from those in the standard k-ε model, and additional terms and functions in the transport equations for k and ε are written as follows:

$$\frac{\partial}{\partial t}(\rho k) + \frac{\partial}{\partial x_i}(\rho k u_i) = \frac{\partial}{\partial x_j}\left(\alpha_k \mu_{eff} \frac{\partial k}{\partial x_j}\right) + G_k + G_b - \rho\varepsilon - Y_M + S_k \quad \text{(II.25)}$$

$$\frac{\partial}{\partial t}(\rho \varepsilon) + \frac{\partial}{\partial x_i}(\rho \varepsilon u_i) = \frac{\partial}{\partial x_j}\left(\alpha_\varepsilon \mu_{eff} \frac{\partial \varepsilon}{\partial x_j}\right) + \frac{\varepsilon}{k} C_{1\varepsilon}(G_k + C_{3\varepsilon} G_b) - C_{2\varepsilon}\rho \frac{\varepsilon^2}{k} - R_\varepsilon + S_\varepsilon \quad \text{(II.26)}$$

Where:

G_k : Generation of turbulence kinetic energy due to the mean velocity gradient.

G_b: Generation of turbulence kinetic energy due to buoyancy.

Y_M : Contribution of the fluctuating dilatation in compressible turbulence to the overall dissipation rate.

The quantities α_k and α_ε are the inverse effective Prandtl numbers for k and ε, respectively.

S_k and S_ε are user-defined source terms. The scale elimination procedure in RNG theory results in a differential equation for turbulent viscosity:

$$d\left(\frac{\rho^2 k}{\sqrt{\mu\varepsilon}}\right) = 1.72\frac{\hat{V}}{\sqrt{\hat{V}^3 - 1 + C_V}}d\hat{V} \quad \text{(II.27)}$$

Where:

$$\hat{V} = \frac{\mu_{eff}}{\mu} \quad \text{(II.28)}$$

$$C_V \approx 100 \quad \text{(II.29)}$$

Equation (II.22) is integrated to obtain an accurate description of how the effective turbulent transport varies with the effective Reynolds number (or eddy scale), allowing the model to better handle low-Reynolds-number and near-wall flows.

The constants of the RNG-k-ε turbulence model is presents in table II.3.

Table II.3. Constants of the RNG-k-ε turbulence model.

$C_{1\varepsilon}$	$C_{2\varepsilon}$	C_μ	η_0	β
1.42	1.68	0.0854	4.38	0.012

II.8.2. k-ω (k-omega) Model

The standard k-ω (k-omega) turbulence model is a widely used two-equation turbulence model in Computational Fluid Dynamics (CFD). It aims to accurately predict turbulent flows by solving transport equations for turbulent kinetic energy (k) and specific dissipation rate (ω).

In the k-ω standard model, the transport equations of the specific dissipation rate ω and the turbulent kinetic energy k and are written as follows:

$$\frac{\partial}{\partial t}(\rho k) + \frac{\partial}{\partial x_i}(\rho k u_i) = \frac{\partial}{\partial x_i}\left(\Gamma_\omega \frac{\partial k}{\partial x_j}\right) + G_k - Y_k + S_k \quad \text{(II.30)}$$

$$\frac{\partial}{\partial t}(\rho \omega) + \frac{\partial}{\partial x_i}(\rho \omega u_i) = \frac{\partial}{\partial x_j}\left(\Gamma_\omega \frac{\partial \omega}{\partial x_j}\right) + G_\omega - Y_\omega + S_\omega \quad \text{(II.31)}$$

Table II.4. illustrates the different constants employed in the k-ω model.

Table II.4. Constants of the standard k-ω (k-omega) model.

α_0	α_∞	α^*_∞	R_ω	R_k	σ_k	σ_ω
1/9	1.9	1.0	2.95	6.0	2.0	2.0

II.9.Discrete Ordinates (DO) radiation model

The Discrete Ordinates (DO) radiation model is a widely used approach in Computational Fluid Dynamics (CFD) for simulating radiative heat transfer in participating media. It is based on the discretization of the radiation intensity over discrete solid angles (ordinates) and is particularly suitable for solving problems involving non-isotropic radiation fields and complex geometries.[19]

Two implementations of the DO model are available in ANSYS Fluent: uncoupled and (energy) coupled. The uncoupled implementation is sequential in nature and uses a conservative variant of the DO model called the finite-volume scheme and its extension to unstructured meshes. In the uncoupled case, the equations for the energy and radiation intensities are solved one by one, assuming prevailing values for other variables.

The DO model considers the radiative transfer equation (RTE) in the direction $\vec{s}$ as a field equation. [1]

$$\nabla.(I(\vec{r},\vec{s})\vec{s}) + (a+\sigma_s)I(\vec{r},\vec{s}) = an^2\frac{\sigma T^4}{\pi} + \frac{\sigma_s}{4\pi}\int_0^{4\pi} I(\vec{r},\vec{s}')\Phi(\vec{s},\vec{s}')\,d\Omega' \qquad \text{(II.32)}$$

ANSYS Fluent also allows the modeling of non-gray radiation using a gray-band model. The RTE for the spectral intensity $I_\lambda(\vec{r},\vec{s})$ can be written as :

$$\nabla.(I_\lambda(\vec{r},\vec{s})\vec{s}) + (a_\lambda+\sigma_s)I_\lambda(\vec{r},\vec{s}) = a_\lambda n^2 I_{b\lambda} + \frac{\sigma_s}{4\pi}\int_0^{4\pi} I_\lambda(\vec{r},\vec{s}')\Phi(\vec{s},\vec{s}')\,d\Omega' \qquad \text{(II.33)}$$

Here λ is the wavelength, a_λ is the spectral absorption coefficient, and $I_{b\lambda}$ is the black body intensity given by the Planck function. The scattering coefficient, the scattering phase function, and the refractive index n are assumed independent of the wavelength.

The non-gray DO implementation divides the radiation spectrum into N wavelength bands, which need not be contiguous or equal in extent. The wavelength intervals are suppliedand correspond to values in vacuum ($n = 1$). The RTE is integrated over each wavelength interval, resulting in transport equations for the quantity $I_\lambda\,\Delta\lambda$, the radiant energy contained in the wavelength band. The behavior in each band is assumed gray. The black body emission in the wavelength band per unit solid angle is written as follow:

$$[F(0 \to n\lambda_2 T) - F(0 \to n\lambda_1 T)]n^2 \frac{\sigma T^4}{\pi} \quad \text{(II.34)}$$

Where $F(0 \to n\lambda T)$ is the fraction of radiant energy emitted by a black body in the wavelength interval from 0 to λ at temperature T in a medium of refractive index. λ_2 and λ_1 are the wavelength boundaries of the band.

The total intensity $I(\vec{r}, \vec{s})$ in each direction $\vec{s}$ at position $\vec{r}$ is computed using:

$$I(\vec{r}, \vec{s}) = \sum_k I_{\lambda_k}(\vec{r}, \vec{s})\Delta\lambda_k \quad \text{(II.35)}$$

Where the summation is over the wavelength bands.

Boundary conditions for the non-gray DO model are applied on a band basis. The treatment within a band is the same as that for the gray DO model.[1]

II.10. Conclusion

In this chapter, we have presented the basic equation for numerical method in the computational fluid dynamic and we have given some definition for a CFD code and how to choose the appropriate mesh for any structure. More than this,we have given some definition and formulation for the turbulence models used like Standard k-ε, Realizable k-ε, RNG k-ε, and k-ω model.

Chapter III

″Results and discussion″

III.1. Introduction

The extensive consumption of the fossils fuel sources and growth of the pollution rate leads human to find renewable resources. Among these resources, solar thermal technologies are efficient a system harnesses the heat from the sun to produce electricity. Specifically, Solar Chimney Power Plant (SCPP) is a mean of power generation from the solar energy. One of the main benefits of the solar chimney power plant is its limited compounds. It comprises four mainly parts which are the collector, the chimney, the turbine and the transition element. The transition element is an important zone, which is the location of the flow direction change. It is typically consists of the chimney junction and the guide wall. A schematic of the SCPP compositions is shown in figure III.1. The SCPP system is based on both phenomena as the greenhouse effect and the natural convection under the transparent roof of the collector. The solar radiation absorbed by the ground (absorber) is converted into heat energy and emitted again to the collector roof. In fact, the air receives both the energy types liberated by the ground. When the air is heated, its density is decreases. Then an airflow is created inside the chimney to make a pressure gradient between the inlet and the outlet of the tower. The hot air is moved and raised at the tower to turn a turbine that is coupled with an electric generator [1]. This parts aims to examine the effect of the chimney junction radius on the turbulent airflow inside a solar chimney power plant. Using the commercial software "ANSYS Fluent", the thermodynamic and the turbulence characteristics are presented for different configurations. With the same chimney and collector dimensions, two-junction radius are investigated. The benefit of using the CFD method is expected to its accuracy and high capacity.

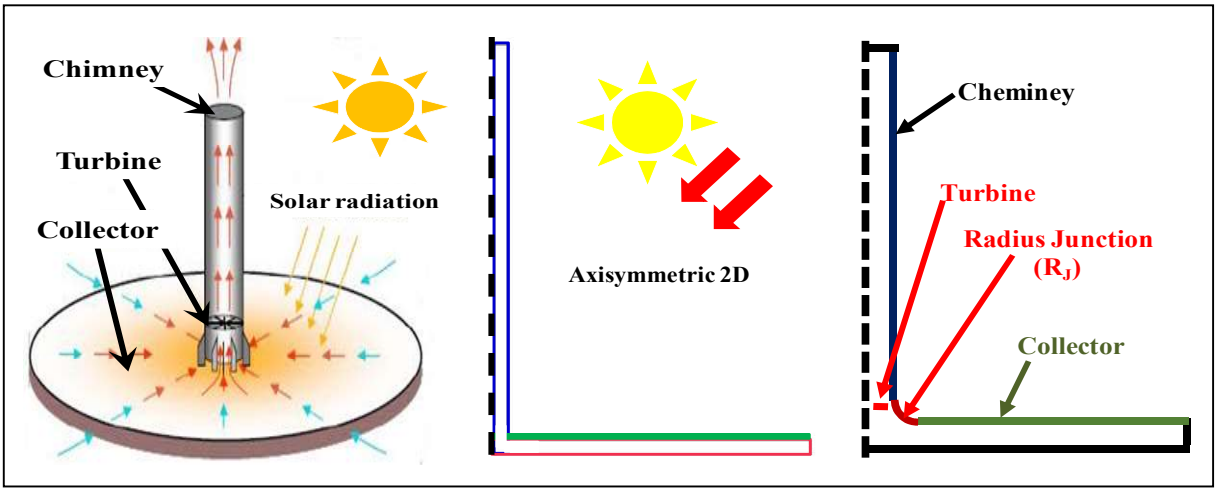

Figure III.1. SCPP compounds

III.2. Methodology

Ansys Fluent is a computer program used the Finite Volume Method (FVM) to solve the mathematical model which is defined the studied problem. To prepare a full simulation, numerous steps must be followed. A simple schematic presented these steps is shown in figure III.2. [12]

- **Step1.**Creation of the geometry (Physical model). The inputs for this interface are x and y coordinates of all the points that defined the geometry of the SCPP. Indeed, incorporation of the different parameters for the physics interfaces of the geometry. In fact, boundary conditions are defined.
- **Step2.**Creation of the mesh grid. A user-controlled mesh is built automatically. Indeed, the element size parameters and free quad settings are applied. The diagram, nominated upwind, is used for all discretization parameters.
- **Step3.**Configuration to minimize the simulation error, the convergence criteria is fixed to 10^{-6} for all residuals values.
- **Step4.** A default solver sequence is defined to compute the distribution of the velocity, temperature and static pressure.

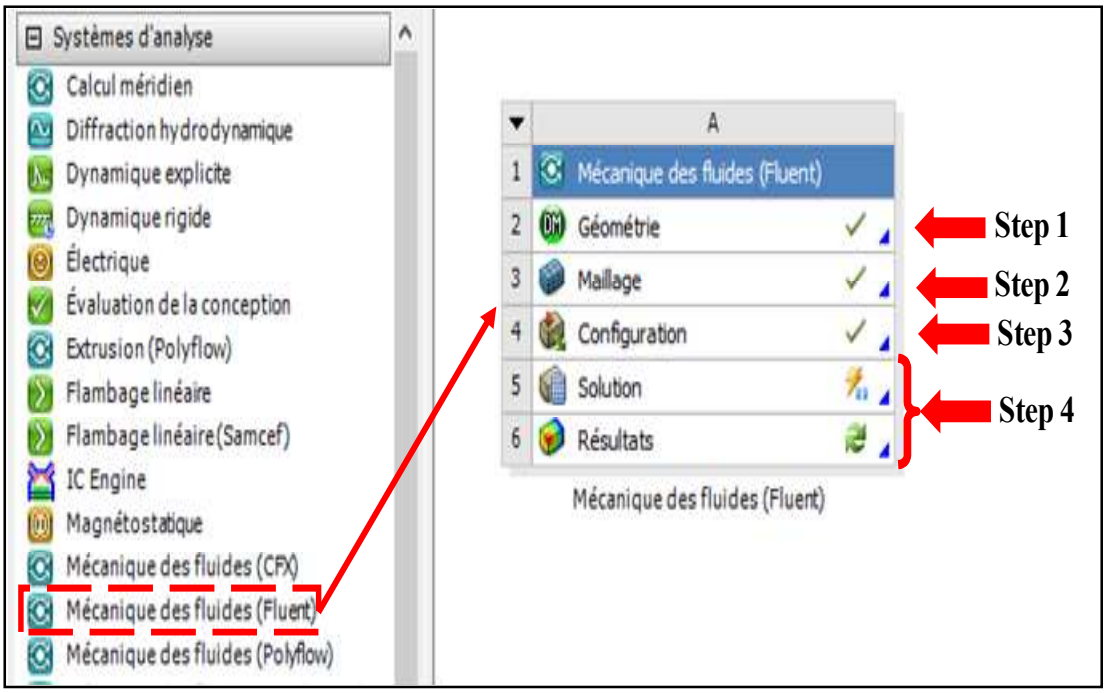

Figure III.2. The structure identifying the main steps for the Ansys fluent model creation

III.2.1. Computational domains

To examine the impact of the chimney junction radius on the local airflow characteristics, four configurations with different junction radius, R_J=0 m, R_J=0.05 m, are carried out. Figure III.3 shows the different considered configurations. The first one is similar to the experimental prototype.[24] However, the other configurations are giving by varied junction radius.

In all cases, the chimney height is equal to H_{ch}=2.9 m, the chimney diameter is equal to D_{ch}=0.16 m, the collector height is equal to H_c=0.1 m and the collector diameter is equal to D_c=3.7 m. The important step to acquire a useful and correct simulation is the manufacturing of the meshing grid. Based on an anterior study of the meshing effect on the behavior of the airflow inside the SCPP system, the best meshing type to model the different geometries is the quadratic and structured meshing. [24]

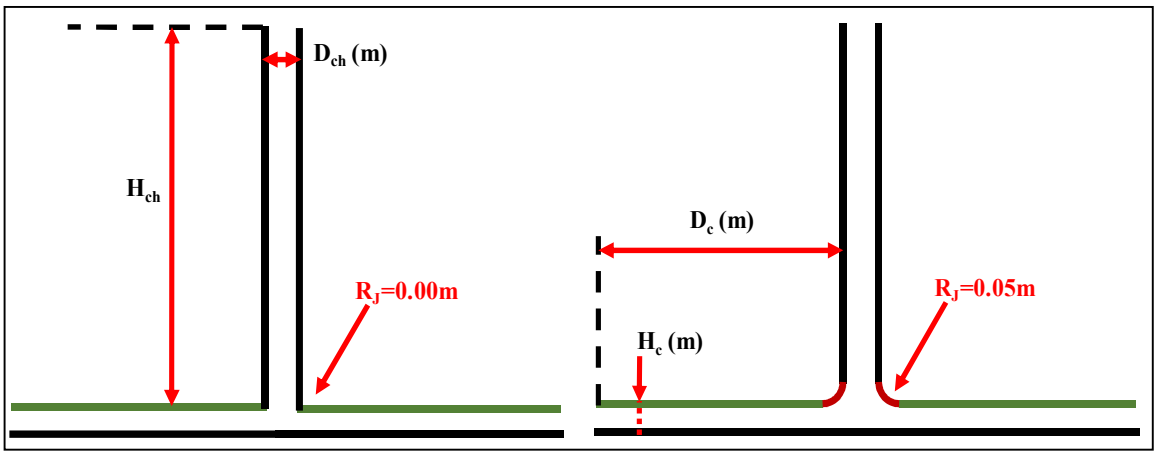

Figure III. 3. Proposed configurations

Figure III.4 shows the applied meshing grid of the configuration with junction radius equal to R_J=0.00 m. An essential process in simulation, mesh creation (or meshing), directly influences model convergence and analysis accuracy. This study uses structural quadrature cells to mesh the SCPP's 2D full domain. To enhance the calculation stability, finer cells are created near the walls. For all cases, the minimum cell size is equal to 1 mm.

As a result, the third mesh defined by 41 294 is selected as the best one because it is compared with reference [1]. After meshing optimization, it is believed that the most efficient numerical model will be a useful tool for analyzing the impacts of suggested designs in a solar power plant chimney flow.

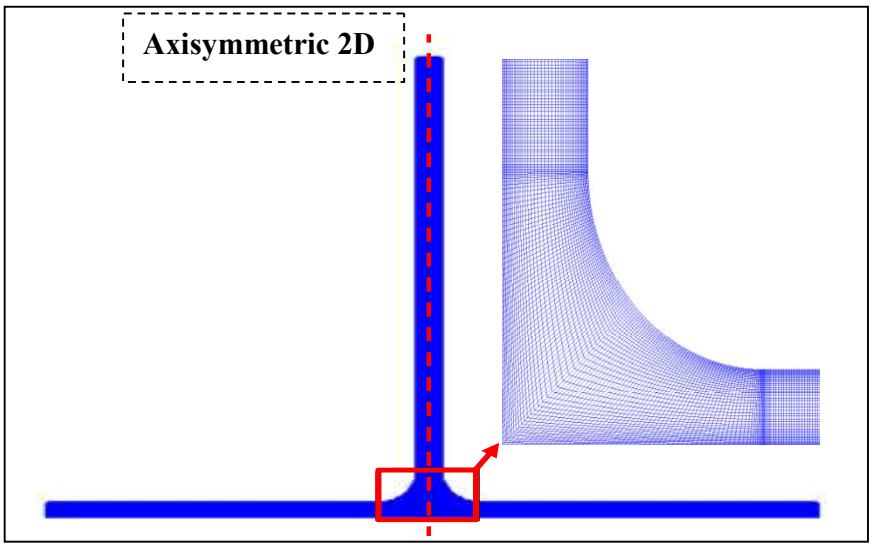

Figure III.4. Meshing grid.

III.2.2. Boundary conditions

The applied boundary conditions are shown in figure III.5. By incorporation of the DO radiation model, the collector roof is defined as a semi-transparent wall.

Collector inlet	p = 101325 Pa T_0 = 308 K
Chimney outlet	p = 101325 Pa
Collector wall	h = 8 $W.K^{-1}.m^{-2}$ T_0 = 308 K
Chimney wall	Q = 0 $W.m^{-2}$
Absorber wall	h = 8 $W.K^{-1}.m^{-2}$ T_0 = 308 K

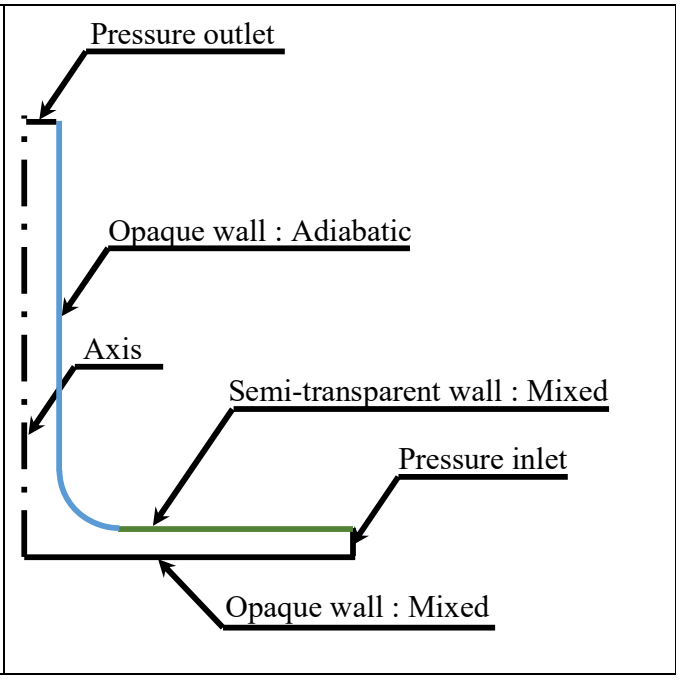

Figure III.5. Boundary conditions.

The chimney, the junction and the absorber are defined as opaque walls. For the thermal boundary conditions, both convection and radiation heat transfer mode are applied on the absorber and the collector walls.

These conditions revealed the air heating process by greenhouse effect. This type of boundary condition is named “mixed”.

However, the other walls are taken as adiabatic walls. The various sun irradiation values and its anticipated beam direction are displayed in Table III.1 at 13:00.[1]

Table III.1. Radiations conditions. [1]

Solar irradiation	Direct	880
	Diffuse	83.3
Beam direction	Chimney axis	0.946
	Collector axis	0.152

III.3. Numerical results

After conducting extensive analysis, the numerical results are in, providing a comprehensive snapshot of our findings. These results guiding us towards informed decisions and future endeavors.

III.3.1. Temperature

The temperature distributions in the full domain of the solar chimney for the different junction radii, R_J=0 m, and R_J=0.05 m are shown in figure III.6.

According to these results, it can be seen that the change of junction radius have a slightly effect on the temperature distribution. For all the cases, the temperature is equal to the ambient value, equal to T_0=310 K, at the SCPP inlet.

Then, a considerable gradient appears between the inlet and the collector outlet. In the chimney region, the airflow remains hot due to the adiabatic proposed chimney and the small altitude.

Otherwise, the temperature features significant values near the absorber wall which is closely equal to T=331K for all considered configurations.

This fact could be understood by the impact of the chimney junction only on the dynamic characteristics inside the SCPP system.

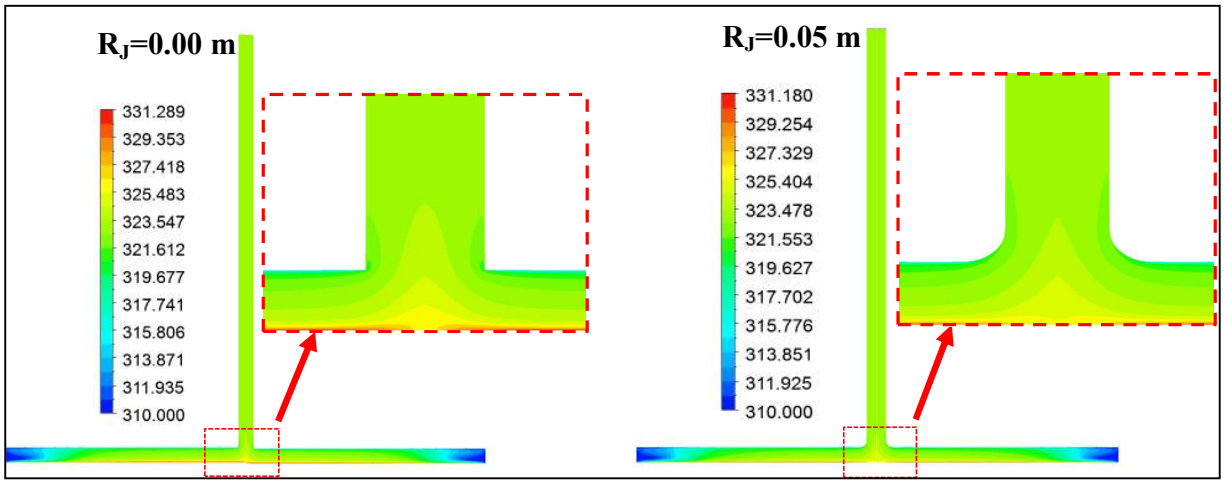

Figure III.6. Temperature distribution.

III.3.2. Magnitude velocity

The distributions of the magnitude velocity in the full domain of the solar chimney for the different junction radii, R_J=0.00 m, and R_J=0.05 m, are shown in figure III.7. From these results, it can be seen that the change of the junction radius affects the magnitude velocity in distributions and values. In fact, the acceleration zone is located at the chimney inlet for the standard chimney configuration (R_J=0.00 m), while the air velocity accelerates at the chimney outlet in the configurations with junction element. In the first case, the magnitude velocity roses continuously from the collector inlet to the SCPP center, then a peak of 1.189 $m.s^{-1}$ is shown near the chimney inlet. Following a slight fall above the chimney inlet, the magnitude velocity leveled off and remained constant along the chimney. For the three other configurations, the air velocity present the same behavior with the standard solar chimney in the collector, while a gradual rise in the magnitude velocity appears from the junction element to the chimney exit. Indeed, it is clear that the peak zone is modified when increasing the junction radius. In the meantime, the maximum value of the magnitude velocity increases with the junction radius due to the reduction of the friction loss in the transition zone. In these conditions, it is equal to V=1.189 $m.s^{-1}$ for the first case, and V=1.248 $m.s^{-1}$ for the second case.

Although, the maximum and the average velocity for R_J=0 m are almost equals. The maximum value of the magnitude velocity for the second junction radius R_J=0.05 m is higher than the one of first case. However, the values at the chimney inlet are very low in the solar chimney with a junction element. These results are confirmed by figure III.7.

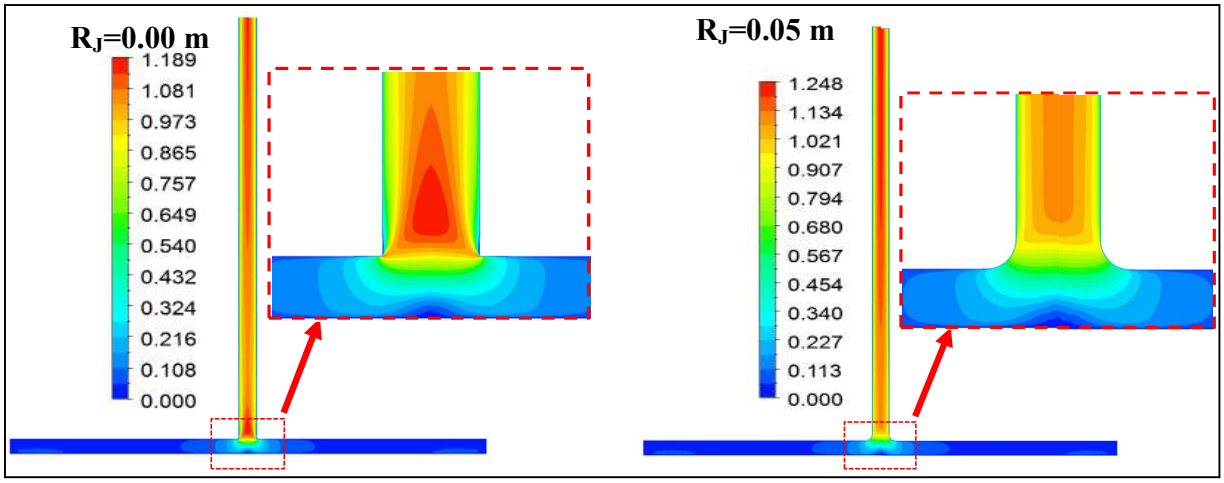

Figure III. 7. Magnitude velocity distribution

III.3.3. Pressure

The distributions of the static pressure in the full domain of the solar chimney for the different junction radii, R_J=0.00 m, and R_J=0.05 m, are shown in figure III.8. From these results, it has been noted that similar to the magnitude velocity distribution, the static pressure distribution varies from one configuration to another.

In fact, the static pressure is approximately remained constant under the collector and then a slow decrease is shown at the collector outlet. The static pressure plummets steeply throughout the transition section when the air changes it. Then, a gradual rise along the chimney is shown to reach the ambient pressure at the chimney outlet. It is clear that the depression zone upsurges with the increase of the junction radius. The small depression area is shown in the first configuration, while a large area appears in the fourth configuration. In fact, the chimney junction could make an enlargement in the depression zone, which presents a good agreement for turbine power.

However, the lowest value of the relative static pressure increases with the increase of the junction radius. In these conditions, it is equal to p=-1.569 Pa for the first case, p=-0.772 Pa and for the second case, p=-0.675 Pa.

The total pressure is the sum of the static and the dynamic pressures. The pressure extracted by the turbine is a part of the total pressure at the turbine location. Indeed, the total pressure is an informative parameter for the turbine energy input.

Figure III.9 shows the distribution of the static pressure in the full domain of the solar chimney for the two studied configurations. It is clear from this figure that the static pressure presents the same distribution shape in all cases. It is roughly constant in the collector and it increases progressively along the chimney to reaches the ambient pressure at the chimney outlet. The difference between the two cases is shown in the weakest values.

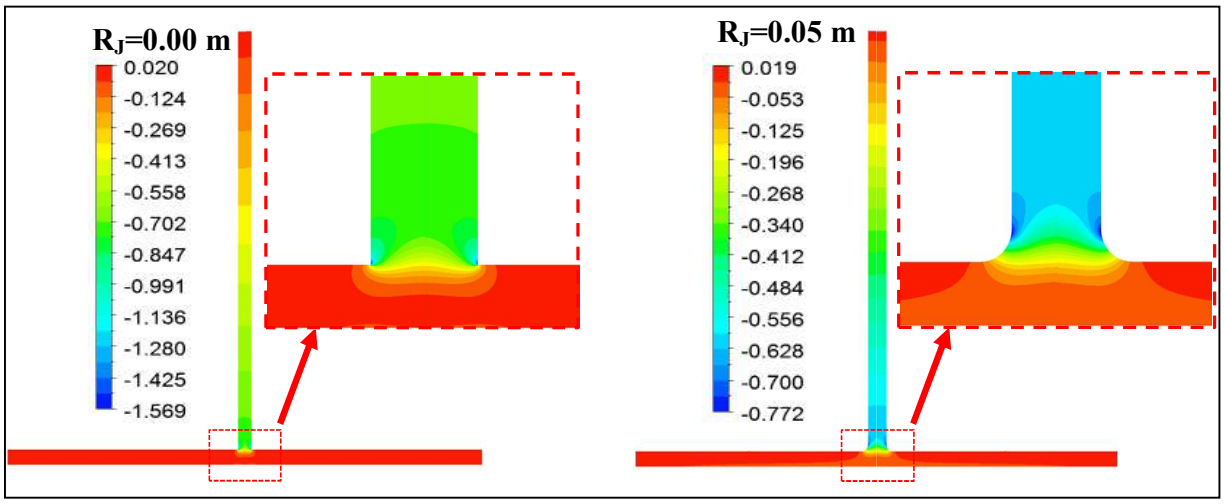

Figure III.8. Static pressure distribution

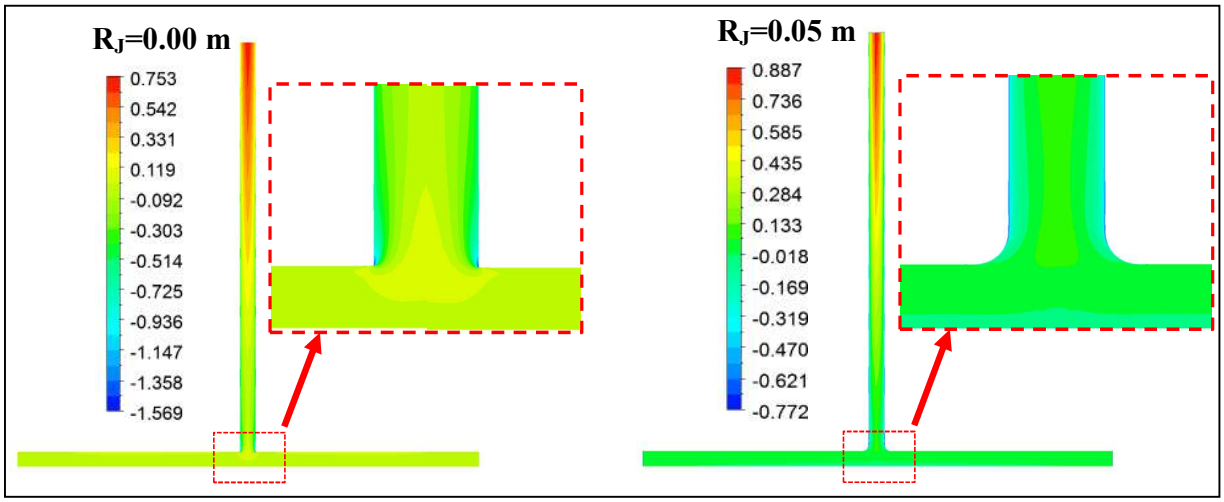

Figure III.9. Total pressure distribution

III.4. Conclusion

In this chapter, the effect of the junction radius on the SCPP performance is carried out. The local airflow characteristics are analyzed for four junction radius; R_J=0.00 m, and R_J=0.05 m.

The findings showed that:

Advantageously, the maximum velocity values are localized at the chimney inlet for the small junction radius (R_J=0.00 m) which presents a benefit solution to install the turbine near the ground. A negligible dissipation rate of the turbulent kinetic energy was appeared for the most large junction radius.

From this study, it has been noted that the solar chimney power plant without junction part has a good agreement in terms of structure and operation cost. However, the SCPP with typical junction presents an efficient device in terms of energetic efficiency.

"General Conclusion"

General Conclusion

The performance of the SCPP is investigated in this study in relation to the junction radius. Analysis of the four junction radius local airflow characteristics.

In this master's memory, an investigation into the impact of junction radius on the performance of the Solar Chimney Power Plant (SCPP) is conducted. The local airflow characteristics are examined for four different junction radii: RJ=0.00 m and RJ=0.05 m.

The results revealed the following, interestingly, the highest velocity values are concentrated at the chimney inlet for the smallest junction radius (RJ=0.00 m), suggesting an advantageous placement for turbine installation near the ground. Conversely, a minimal dissipation rate of turbulent kinetic energy was observed for the largest junction radius.

This study highlights that the SCPP without a junction segment demonstrates favorable agreement concerning both structural integrity and operational cost. However, the SCPP equipped with standard junction exhibits enhanced energy efficiency.

In practical terms, understanding how the chimney junction radius affects airflow is crucial for optimizing the design and performance of SCPPs in real-world settings. The observed changes in local airflow characteristics have direct implications for turbine site selection, structure design, and power capacity. For instance, a specific chimney junction radius may result in more efficient airflow distribution within the chimney, positively impacting turbine performance and, subsequently, power generation.

This knowledge is pivotal for engineers and designers working on SCPP projects, providing them with insights to make informed decisions about chimney design parameters.

Recommendations for future research

- Explore the influence of ambient wind conditions on the performance of the solar chimney.
- Conduct a comprehensive economic viability assessment of SCPPs with varying chimney junction radii. Consider factors such as initial costs, maintenance, and long-term operational expenses to provide a holistic view of the technology's feasibility.

- Investigate the use of advanced numerical modeling techniques beyond ANSYS Fluent, considering emerging technologies or methodologies that may provide more accurate predictions of airflow dynamics and system performance.

These recommendations aim to enhance the current work and suggest exciting avenues for future research in the field of Solar Chimney Power Plants.

"References"

References

[1] H. Nasraoui, H. Benguesmia, B. Bakri, Z. Driss, H. Kchaou, “Impact of the chimney junction radius on the airflow characteristics inside a solar chimney power plant”. Thermal Science, First online, 2024.

[2] B. Bakri, H. Benguesmia, H. Nasraoui, Z. Driss, “Experimental Study of Solar Chimney Power Plant”, Journal of Advanced Research in Fluid Mechanics and Thermal Sciences, Vol.101(1), pp.207–214, 2023.

[3] A. Laghzaoui, D. Peerhossaini, “Stockage de chaleur: Energie solaire et autre application. Rapport interne”, Ecole des mines de Douai, France, 2010.

[4] C. Djassem, “Réalisation et expérimentation d'une cheminée solaire”, Mémoire de Master, Université Kasdi Merbah, Ouargla, 2014.

[5] M. GEEF, E. Cota, “Solar energy, renewable energy and the environment”, CRC Press, New York, USA, 2010.

[6] M. Antoine, “Contribution à la conception et à l’optimisation thermodynamique d’une Microcentrale solaire Thermo électrique”, Thèse de doctorat en mécanique énergétique, Université de lorraine, 2012.

[7] K. Meliani, A. Taghourt, “Analyse des Performances énergétiques d’une Centrale à Cheminée Solaire par une prise en charge du stockage thermique”, Mémoire de fin d’étude, Ecole nationale polytechnique, Juin 2015.

[8] T. Chergui, H. Boualit, S. Larbi, A. Bouhdjar, “Technologie de la cheminée solaire pour la production de l’énergie Revue des Energies Renouvelables SIENR’12 Ghardaïa, pp.83-94, 2012.

[9] I. Cabanyes, “Las chimeneas solares (Solar chimneys)”, La ernergia eléctrica. Cited due to Wikipedia; 1903.

[10] C.B. Maia, A.G. Ferreira, R.M. Valle, M.F.B. Cortez, “Theoretical Evaluation of the Influence of Geometric Parameters and Materials on the Behavior of the Airflow in a Solar Chimney”, Computers and Fluids, Vol. 38, N°3, pp. 625-636, 2009.

[11] R.E. Lucier, “Apparatus for converting solar to electrical energy”, US. Patent, 1979.

[12] C. Djassem, “Réalisation et expérimentation d'une cheminée solaire”, Mémoire de Master, Université Kasdi Merbah, Ouargla, 2014.

[13] C. Ketlogetswe, J.K. Fiszdon, O. Seabe, "Solar Chimney Power Generation Project-The Case for Botswana", International Journal of Renewable and Sustainable Energy Review, Vol.12, N°7, pp. 2005-2012, 2008.

[14] J. Schlaich, "The Solar Chimney", Edition Axel Menges, Stuttgart, 1995.

[15] B. Mebarki, B. Draoui, B. Allaoui, M. Djilali, L. Rahmani, Etude analytique d'une tour solaire à effet de cheminée destinée pour la production d'énergie électrique au sud ouest de l'Algérie, International Conference en Electrical Engineering, (CIGE'2013), 17-19 November 2013, Bechar, Algeria.

[16] E. Bilgen, J. Rehault, "Solar chimney power plants for high latitudes", Solar Energy, 79, pp. 449-458, 2005.

[17] https://abcnews.go.com/Technology/solar-power-giant-arizona-tower-planned-generate-clean/story?id=14163138

[18] H. Benguesmia, B. Bakri, Z. Driss, A. Ketata, S. Driss, "Effect of the turbulence model on the heat ventilation analysis in a box prototype", Diagnostyka, vol. 21, no. 3, 2020, pp. 55-66.

[19] B. Bakri, H. Benguesmia, A. Ketata, S. Driss, Z. Driss. "Choice of the appropriate turbulence model for modeling the air flow inside a room." In 1ère Conférence National sur: la Transition Énergétique en Algérie Conférence. M'sila, Algeria, 2020.

[20] A. Ayadi, A. Bouabidi, Z. Driss, H. Nasraoui, M. Bsisa, M.S. Abid, "Study of the Turbulence Model Effect on the Airflow Characteristics Inside a Solar Chimney Power Plant". In: Driss, Z., Necib, B., Zhang, HC. (eds) CFD Techniques and Energy Applications. Springer, Cham, 2018.

[21] H. Nasraoui, Z. Driss, H. Kchaou, "Effect of the chimney design on the thermal characteristics in solar chimney power plant", Journal of Thermal Analysis and Calorimetry, Vol.140,pp.2721–2732, 2020.

[22] H. Nasraoui, Z. Driss, H. Kchaou, "Theoretical Study of the Geometrical Parameters Effect on the Behavior of a Solar Chimney Power Plant", In book: Mechanical Engineering Technologies and Applications: Vol.2, pp.129-145, 2023.

[23] H. Nasraoui, A. Bouabidi, Z. Driss, H. Kchaou, "Impact of Venturi Shape on Performance of Solar Chimney Power Plant", In book: Advances in Materials, Mechanics and Manufacturing II, pp.317-325, 2022.

[24] M. Ghalamchi, A. Kasaeian, M. Ghalamchi, A.H. Mirzahosseini, "An experimental study on the thermal performance of a solar chimney with different dimensional parameters", Renewable Energy, Vol.91, pp477-483, 2016.